International Journal for Parasitology 49 (2019) 1061–1073

Contents lists available at ScienceDirect

International Journal for Parasitology

journal homepage: www.elsevier.com/locate/ijpara

Meloidogyne incognita (Nematoda: Meloidogynidae) sterol-binding protein Mi-SBP-1 as a target for its management

Tagginahalli N. Shivakumara [a], Vishal Singh Somvanshi [a,*], Victor Phani [a], Sonam Chaudhary [a], Alkesh Hada [a], Roli Budhwar [b], Rohit Nandan Shukla [b], Uma Rao [a,*]

[a] Division of Nematology, ICAR-Indian Agricultural Research Institute, New Delhi 110012, India
[b] Bionivid Technology Private Limited, 209, 4th Cross, Kasturi Nagar, Bangalore 560043, India

ARTICLE INFO

Article history:
Received 8 April 2019
Received in revised form 16 September 2019
Accepted 19 September 2019
Available online 14 November 2019

Keywords:
Lipogenesis
Management
Meloidogyne incognita
Mi-sbp-1
Parasitism
Target

ABSTRACT

Meloidogyne incognita is a polyphagous plant-parasitic nematode that causes considerable yield loss in agricultural and horticultural crops. The management options available for *M. incognita* are extremely limited. Here we identified and characterised a *M. incognita* homolog of *Caenorhabditis elegans* sterol-binding protein (Mi-SBP-1), a transcriptional regulator of several lipogenesis pathway genes, and used RNA interference-mediated gene silencing to establish its utility as a target for the management of *M. incognita*. *Mi-sbp-1* is predicted to be a helix-loop-helix domain containing DNA binding transcription factor, and is present in the *M. incognita* genome in three copies. The RNA-Seq analysis of *Mi-sbp-1* silenced second stage juveniles confirmed the key role of this gene in lipogenesis regulation in *M. incognita*. In vitro and host-induced gene silencing of *Mi-sbp-1* in *M. incognita* second stage juveniles resulted in loss of nematodes' ability to utilise the stored fat reserves, slower nematode development, and reduced parasitism on adzuki bean and tobacco plants. The multiplication factor for the *Mi-sbp-1* silenced nematodes on adzuki bean plants was reduced by 51% compared with the control nematodes in which *Mi-sbp-1* was not silenced. Transgenic expression of the double-stranded RNA construct of the *Mi-sbp-1* gene in tobacco plants caused 40–45% reduction in *M. incognita* multiplication, 30–43.8% reduction in the number of egg masses, and 33–54% reduction in the number of eggs per egg mass compared with the wild type control plants. Our results confirm that *Mi-sbp-1* is a key regulator of lipogenesis in *M. incognita* and suggest that it can be used as an effective target for its management. The findings of this study can be extended to develop methods to manage other economically important parasitic nematodes.

1. Introduction

Plant-parasitic nematodes (PPNs) are considered to be a serious threat to global food security. They cause an estimated crop loss of approximately 14.6% in tropical and sub-tropical countries and up to 8.8% in developed countries (Nicol et al., 2011), amounting to approximately US $173 billion per year (Elling, 2013). The root-knot nematodes (RKNs; *Meloidogyne* spp.) are the most prevalent and destructive PPNs (Jones et al., 2013). *Meloidogyne incognita* is a widespread and economically important RKN species, having a broad host range and high reproduction rate (Jones et al., 2013). Its life cycle consists of six developmental stages, i.e., egg, 1st stage juvenile (J1), J2, J3, J4 and adult female or male (Hussey, 1985). J2 is the infective stage that penetrates the host root and initiates formation of a permanent feeding site, known as 'giant cell' (Hussey, 1985), which serves as a specialised nutrient sink and supplies nutrients to the developing nematode. The J2 subsequently moults to J3, J4 (both non-feeding stages) and eventually into either an adult female which continues to feed, enlarge and reproduce or a male (Kyndt et al., 2013).

Despite the fact that PPNs are a serious threat to crops, there is an acute scarcity of management options for these parasites. Most of the chemical pesticides used for PPN management are general biocides or insecticides which have either been banned or phased out due to their ill effects on the environment (Collange et al., 2014; Kim et al., 2017). At present, only four chemicals, fluopyram (Faske and Hurd, 2015), fluensulfone (Kearn et al., 2014), fluazaindolizine (Lahm et al., 2017) and tioxazafen (Slomczynska et al., 2014) are registered as 'nematicides' for PPN management, which emphasizes the urgent need for newer nematode management options and strategies. However, the discovery of a new drug and

* Corresponding authors.
E-mail addresses: vssomvanshi@iari.res.in (V.S. Somvanshi), umarao@iari.res.in (U. Rao).

https://doi.org/10.1016/j.ijpara.2019.09.002
0020-7519/

developing it into a ready-to-use finished product is a highly expensive and time-consuming process (Hughes et al., 2011).

Recent advancements in PPN genomics and transcriptomics have made it possible to identify promising molecular targets and metabolic choke points that may be exploited for their management through transgenic approaches or target-based drug discovery (Foster et al., 2005; Mitreva et al., 2007; Danchin et al., 2013; Taylor et al., 2013; IHG consortium, 2019). Lipid metabolism is highly conserved across the Phylum Nematoda (Watts and Ristow, 2017), and several lipid metabolism pathway genes have shown potential as targets for nematode management (Ashrafi et al., 2003; Kumar et al., 2007; Taylor et al., 2013). A total of 471 putative lipid metabolism genes have been identified in *Caenorhabditis elegans* (Zhang et al., 2013), and worm mutants defective in fat synthesis are known to stop feeding, with reduced physical activity (You et al., 2008; Hyun et al., 2016). Unlike most other animals, *C. elegans* can synthesise a range of monomethyl and polyunsaturated fatty acids (PUFA) de novo, using acetyl-CoA or isobutyryl-CoA as precursors (Wallis et al., 2002). The syntheses include a complex nexus of pathways involving several genes and enzymatic actions (Watts and Browse, 2002; Rappleye et al., 2003; Chirala and Wakil, 2004; Kniazeva et al., 2004; Entchev et al., 2008; Branicky et al., 2010; Zhang et al., 2011; Watts and Ristow, 2017). The PUFAs (fatty acids with more than one double bond in their backbone) are important for nematode growth, reproduction, neurotransmission and signalling, whereas the neutral lipids such as triacylglycerols serve as major storage fats (Watts and Ristow, 2017). The fat deposits are catabolized by lipases, which hydrolyses triglycerol to glycerol and free fatty acids (Lee et al., 2014). The fatty acids are then activated and transported into mitochondria and peroxisomes for production of ATP through a β-oxidation pathway (Reddy and Hashimoto, 2001; Wanders et al., 2010). Although highly conserved amongst nematodes, the lipid metabolism pathway(s) have attracted very little attention as a prospective molecular target for nematode management.

The *C. elegans* sterol regulatory element binding protein (SBP-1) is a homologue of mammalian sterol regulatory element binding protein SREBP-1c, and is known to regulate transcription of genes involved in lipogenesis (e.g. *fat-5*, *fat-6*, *fat-7*, *elo-5*, *elo-6*) and phospholipid synthesis (Kniazeva et al., 2004; Yang et al., 2006; Walker et al., 2010). Silencing of *sbp-1* had detrimental effects on *C. elegans* physiology (McKay et al., 2003; You et al., 2008; Hyun et al., 2016). However, no previous information about the role of *sbp-1* in a PPN is present in the literature. We hypothesized that the *M. incognita* homologue of *C. elegans sbp-1* (hereafter *Mi-sbp-1*) could be used as a target for its management due to its key regulatory role in nematode lipogenesis. Here we identified and characterised *Mi-sbp-1* in *M. incognita*, elucidated its role in the regulation of global gene expression by RNA-Seq, and determined its role in nematode biology, reproduction and plant parasitism using in vitro and host delivered RNA interference (RNAi).

2. Materials and methods

2.1. Identification and sequence analysis of Mi-sbp-1 from M. incognita

The *Mi-sbp-1* gene was identified using the *C. elegans* SBP-1 protein sequence as a query for a BLAST search of WormBase ParaSite (http://parasite.wormbase.org/tools/Blast) and the INRA *Meloidogyne* genomic resource database (http://www6.inra.fr/meloidogyne_incognita/Genomic-resources2/Blast). The retrieved *M. incognita* sequences were analyzed for the presence of conserved domains and motifs using the ExPaSy bioinformatics Resource Portal, PROSITE (http://prosite.expasy.org). The protein secondary structure prediction and modeling were done using SWISS-MODEL (https://swissmodel.expasy.org/). The Mi-SBP-1 (translated) sequence was then subjected to a BLAST search against WormBase ParaSite and UniProt databases to retrieve the homologous sequences from other nematodes, and phylogenetic analysis of the putative nematode SBP-1 protein sequences was done by maximum likelihood analysis using MEGA7 (Kumar et al., 2016). The SBP-1 sequence of *Xenopus tropicalis* was used as an outgroup. Gene-specific primers were designed (http://eu.idtdna.com/Primerquest/Home/Index) to amplify the putative *Mi-sbp-1* sequence from *M. incognita* genomic DNA. Primer details are given in Supplementary Table S1.

2.2. Nematode culture and estimation of fat reserves by Nile-Red staining

A pure culture of *M. incognita* was multiplied on eggplant (*Solanum melongena* cv. Pusa Purple Long) in a greenhouse at Indian Council of Agricultural Research (ICAR) – Indian Agricultural Research Institute (IARI), New Delhi, India. Egg masses were hand picked from the washed roots of 2 months old infected plants and hatched via modified Baermann's assembly (Whitehead and Hemming, 1965) to obtain infective J2s or pre-parasitic J2s. Other developmental stages were dissected out from the plant roots as described earlier (Shivakumara et al., 2017) at suitable intervals for various experiments.

To quantify nematode fat reserves at different time points, various developmental stages of *M. incognita* were extracted from among plant roots and inside the plant roots, and stained using Nile Red stain at 1, 2, 4, 6, 8, 10, 13 and 15 days post inoculation (pi) as described previously (Shivakumara et al., 2018). The fat reserves were quantified by image analysis of the stained nematodes using National Institutes of Health (USA; NIH) software ImageJ version 1.48 (Abràmoff et al., 2004), and the body mass of each nematode was estimated using the formula $[(L \times W^2)/(1.6 \times 10^6)]$ (Andrassy, 1956), where L = body length, W = body width. Statistical significance was determined at $P = 0.01$.

The effect of silencing of *Mi-sbp-1* on reserve fat utilisation was determined by soaking the J2s in *Mi-sbp-1* double-stranded (ds) RNA solution for 6 days (detailed methodology for in vitro RNAi is described below in Section 2.4). The dsRNA solution was replenished every 48 h, and the J2s were subjected to Nile Red staining. The fat reserves of 6 days dsRNA fed/soaked (FD) nematodes were compared with 6 days starved (ST) J2s as well as freshly hatched (FR) J2s. The stained worms were observed on a temporary mount using a 2% agarose pad and photomicrographs were taken using a compound microscope (Zeiss Imager M2m) with fluorescence filter.

2.3. Molecular biology techniques

The genomic DNA (gDNA) was extracted from *M. incognita* J2s using a PureLink Genomic DNA mini kit (Invitrogen, USA) as per the manufacturer's instructions. Total RNA was extracted from the J2s using a NucleoSpin RNA kit (Macherey-Nagel, Düren, Germany), quality and quantity were assessed using a Nanodrop ND-1000 spectrophotometer (Thermo Fisher Scientific, Waltham, MA, USA), and then converted to cDNA as described previously (Shivakumara et al., 2016). The *Mi-sbp-1* gene was amplified from the cDNA using gene-specific primers (Supplementary Table S1), cloned into a pGEM-T Easy vector (Promega, Madison, WI, USA) and the identity of the insert was re-confirmed by Sanger sequencing.

For the copy number analysis by Southern hybridisation, ~8 μg of gDNA were digested overnight by *Eco*RI restriction enzyme (New England Biolabs, Ipswich, MA, USA) at 37 °C in a circulating water

bath. The digested product was resolved on 0.8% agarose gel followed by transferral onto a nitrocellulose membrane (Roche Applied Science, Indianapolis, IN, USA). The probe was synthesized by amplifying an 877 bp *Mi-sbp-1* gene fragment using gene-specific primers (Supplementary Table S1) and a PCR DIG probe synthesis kit II (Roche Applied Science, Indianapolis, IN, USA). Probing, hybridisation and signal detection were carried out as described earlier (Papolu et al., 2013).

The expression of the *Mi-sbp-1* gene in different developmental stages of *M. incognita* was estimated by quantitative real-time PCR (qRT-PCR). Total RNA was extracted from different developmental stages, reverse transcribed to cDNA, and qRT-PCR was carried out using three biological and three technical replicates (Shivakumara et al., 2017) using the primers given in Supplementary Table S1. Expression of the target gene was normalised using 18S rRNA (HE667742) as an internal reference, data was analysed by the $2^{-\Delta\Delta Ct}$ method (Livak and Schmittgen, 2001), and the results were expressed as log2-transformed fold change values ($P = 0.05$). A similar method was used for the quantification of transcripts of lipogenesis pathway genes in other experiments.

2.4. In vitro RNAi of M. incognita by soaking

dsRNA of *Mi-sbp-1* was synthesized by following the methodology described earlier (Shivakumara et al., 2017) and feeding of dsRNA was done by the soaking method (Urwin et al., 2002). The dsRNA of an unrelated gene (*gfp*, HF675000) was used as a non-native negative control. Approximately 1000 freshly hatched J2s were soaked in 0.1 mg ml^{-1} target dsRNA in 100 µl of soaking buffer and incubated for 48 h on a slowly moving rotator in the dark at 28 °C. Post incubation, the J2s were washed thrice with sterile water, total RNA was extracted, reverse transcribed to cDNA, and qRT-PCR analysis was performed with three biological and technical replicates to confirm the knockdown effect.

2.5. RNA sequencing and data analysis

To determine the effect of *Mi-sbp-1* silencing and starvation on the global gene expression profile and fat metabolism pathway genes, the RNA sequencing (RNA-Seq) of (i) 6 days *Mi-sbp-1* dsRNA fed *M. incognita* J2s (FD), (ii) 6 days starved J2s (ST), and (iii) fresh J2s (FR) was carried out using Illumina HiSeq (Phani et al., 2018). Briefly, total RNA was extracted from ~20,000 *M. incognita* J2s with TRIzol reagent (Thermo Fisher Scientific, Waltham, MA, USA) as per the manufacturer's protocol and gDNA contamination was removed by RQ1 RNase-Free DNase treatment (Promega, Madison, WI, USA). RNA integrity was tested on a Bioanalyzer (Agilent Technologies, Santa Clara, CA, USA), and the RNA quality and concentration were determined by using a 1% agarose gel and NanoDrop-1000 spectrophotometer (Thermo Fisher Scientific, Waltham, MA, USA). Two biological replicates were used for each treatment condition, and oligodT beads (Illumina TruSeq RNA Sample Preparation Kit v2) were used to purify mRNA from ~5 µg of total RNA. The purified mRNA was fragmented in the presence of bivalent cations, and first strand cDNA was synthesised using Superscript II reverse transcriptase (Invitrogen, Carlsbad, CA, USA) and random hexamer primers (Invitrogen, Carlsbad, CA, USA). Second strand cDNA was synthesised in the presence of DNA polymerase I and RNaseH following a standard Illumina protocol. The cDNA was cleaned using an Agencourt AMPure XP purification kit (Beckman-Coulter, Brea, CA, USA), amplified, quantified using a Nanodrop spectrophotometer (Thermo Fisher Scientific, Waltham, MA, USA) and checked for quality with a Bioanalyzer (Agilent Technologies, Santa Clara, CA, USA). In total, six libraries were prepared, two each for FD, ST and FR samples. The cDNA libraries were sequenced on the Illumina HiSeq platform by outsourcing to Bionivid Technologies Pvt. Ltd., Bangalore, India.

Here, we used a fast approach to understand the significant biology by mapping the RNA-Seq reads to the already annotated *M. incognita* transcriptome (Somvanshi et al., 2018). The raw transcriptomic data were subjected to quality control by a NGS QC toolkit (Patel and Jain, 2012) and the high-quality reads were quantitated by directly mapping against the INRA *M. incognita* proteome using Kalisto (Bray et al., 2016). Differentially expressed genes (DEGs) between the FD and ST samples were identified by comparison with the FR sample using the DESeq2 package in R version 3.2.5 (Love et al., 2014). The threshold for DEGs was set as |log2 fold-change| $\geq$2.0 and $\leq$−2.0 at $P \leq 0.05$. Identification of unique and overlapping genes within the DEG datasets was determined using the Venny tool (bioinfogp.cnb.csic.es/tools/venny/index2.0.2.html). The DEGs were subjected to significant biology analysis using GO-Elite (Zambon et al., 2012) and the annotated INRA *M. incognita* proteome (Somvanshi et al., 2018). Expression of selected transcripts of carbon and fat metabolism pathways was validated by qRT-PCR following the methodology described above.

2.6. Plant parasitism assays

The effect of varying levels of *M. incognita* J2 fat reserves on nematode infectivity and reproduction was determined by plant parasitism assays using eggplant (da Silva Rocha et al., 2015). The freshly hatched and 2, 4, 6, 8, and 10 days starved J2s (~400 each) were inoculated onto the roots of 25 days old eggplant seedlings in plastic pots containing 200 g of soil and soilrite at a 3:1 ratio, and grown in a greenhouse under controlled conditions. At 30 days pi, parasitic success of nematodes on these plants was determined by recording the number of galls and egg masses per plant, eggs per egg mass and multiplication factor (Papolu et al., 2013). The experiment was done with two biological replicates, each containing five technical replicates.

The effect of *Mi-sbp-1* gene silencing on nematode development was also evaluated by inoculating the dsRNA-soaked *M. incognita* J2s on adzuki bean plants (*Vigna angularis* var. angularis) in CYG germination pouches (Mega International, St Paul, MN, USA). Approximately 100 J2s were inoculated on the tips of each plant root, and the plants were grown in a growth chamber with a 16:8h light:dark photoperiod with 70% relative humidity at 25–28 °C. The developmental assays were carried out by harvesting the set of plants at 2–16 days pi. Roots were stained by the acid fuchsin-NaOCl method (Byrd et al., 1983) and dissected under a stereo zoom binocular to check the developmental progress of *M. incognita*. Photographs were taken by a Zeiss Axiocam MRm microscope. Another set of plants was harvested at 30 days pi, and used for calculation of the multiplication factor based on the number of galls, egg masses and eggs per egg mass. J2s treated with *gfp* dsRNA were used as a control, and statistical significance was determined at $P = 0.05$.

2.7. Host-induced gene silencing of Mi-sbp-1

A partial sequence of *Mi-sbp-1* (926 bp) was PCR-amplified from the pGEM-T clone (described in Section 2.3) and sub-cloned into a pDONR 221entry vector followed by a pK7GWIWG2(I) RNAi Gateway vector in sense and antisense orientations. The pK7GWIWG2 (I) RNAi Gateway ready vector was obtained from the Department of Plant System Biology, Ghent University, Belgium. The construct was transferred into *Agrobacterium tumefaciens* (LBA4404) through electroporation. Primer details are given in Supplementary Table S1.

Tobacco (*Nicotiana tabacum* var. Petit Havana) seeds were surface sterilised with 70% ethanol and 0.01% mercuric chloride followed by rinsing with autoclaved distilled water. The surface sterilised seeds were germinated on half-strength Murashige-Skoog (MS) agar medium with 1.5% sucrose (pH 5.8) and seedlings were grown in a 16:8h light:dark photoperiod. Leaf explants of 1 cm^2 cut from young tobacco plants were used for *Agrobacterium*-mediated transformation. Pre-cultivated tobacco explants were infected with *Agrobacterium* harbouring the *Mi-sbp-1* RNAi construct and the infected explants were transferred to co-cultivation medium followed by kanamycin selection media. Shoots emerging from the explants were excised and sub-cultured for 10–15 days in fresh selection medium, and elongated shoots were further transferred into rooting medium supplemented with 0.1 mg L^{-1} NAA (1-Naphthaleneacetic acid) (Papolu et al., 2013). Plants with well-established roots were hardened and transferred into the transgenic facility at ICAR-IARI, New Delhi, India for further development and production of T_1 seeds. Plants transformed with an empty vector served as the control. Total gDNA was isolated from the leaves of T_1 plants and the presence of the transgene was confirmed by PCR with a set of primers given in Supplementary Table S1. The transgene expression was also confirmed in tobacco plants by qRT-PCR. Total RNA was isolated from the leaves of T_1 plants, ~1 μg of total RNA was reverse transcribed to cDNA, and qRT-PCR was carried out with three biological and three technical replicates. The expression of *Mi-sbp-1* in different events was depicted as average Cycle threshold (Ct) values, by calculating the difference between the Ct mean of the target gene and the housekeeping gene 18S RNA.

Tobacco plants (T_1) harbouring the *Mi-sbp-1* RNAi construct were subjected to nematode parasitism assays. The 2 weeks old T_1 plants were grown in pots containing 200 g of soil and soilrite (3:1), inoculated with ~400 *M. incognita* J2s, and maintained in a growth chamber under the above-mentioned conditions. Plants were harvested at 35 days pi, and the nematodes' parasitic success was determined as described previously (Papolu et al., 2013; Shivakumara et al., 2017). Additionally, ~50 females were dissected out from the transgenic plants and measurements (length and width) were obtained to check the morphological aberration (if any) and compared with the control.

3. Results

3.1. Identification and characterisation of M. incognita sbp-1

The homologue of *C. elegans* SBP-1 (Y47D3B.7, 1113 amino acids (aa)) was identified in the *M. incognita* genome sequence, and the 993 aa long *M. incognita* sequence (Minc3s00144g05954; referred to herein as *Mi-sbp-1*) was retrieved as the topmost hit with a total score of 372 at an E-value of 6.83×10^{-111}. The partial nucleotide sequence of *Mi-sbp-1* (2159 bp) was PCR amplified, cloned and re-sequenced for validation (Supplementary Fig. S1A). Re-sequencing and BLAST analysis revealed that the cloned partial *Mi-sbp-1* was 100% identical to the sequence obtained from the *M. incognita* INRA database. Southern blot hybridisation showed the presence of three copies of *Mi-sbp-1* in the *M. incognita* genome (Supplementary Fig. S1B). The characterisation of the predicted protein sequence of Minc3s00144g05954 in the InterPro database suggested the presence of a helix-loop-helix DNA binding domain (IPR036638), and two sterol regulatory element binding protein domains (PTHR12565) (Fig. 1A). The protein modelling by SWISS-MODEL resulted in identification of a template 4atk.1 (microphthalmia-associated helix-loop-helix leucine zipper type DNA binding transcription factor) (Fig. 1B). The evolutionary relatedness of Mi-SBP-1 was analyzed by comparing it with other homologous sequences of animal parasites, plant-parasites and free-living species within the Phylum Nematoda. The maximum likelihood phylogenetic analysis revealed that the SBPs clustered into three groups (shaded yellow boxes in Fig. 1C) as per the trophic groups of the nematodes. The SBPs from PPNs (Clade V; Blaxter et al., 1998) such as *Meloidogyne hapla*, *Meloidogyne javanica*, *Meloidogyne graminicola*, *Meloidogyne floridensis*, *Meloidogyne arenaria*, *Globodera pallida* and *Globodera rostochiensis* clustered together in a single clade whereas the phylogenetic relationships of SBPs from *Ditylenchus destructor* and *Bursaphelenchus xylophilus* were unresolved. The free-living nematode SBPs (Clade IV; Blaxter et al., 1998) clustered together except for *Pristionchus pacificus*. Lastly, the animal parasitic nematode SBPs clustered according to their respective clades, Clade III and Clade V (Blaxter et al., 1998) (Fig. 1C).

3.2. Nematode developmental stage-specific quantitation of lipids and expression of Mi-sbp-1

The lipid content was quantitated at various time points in the life cycle of *M. incognita* by Nile Red staining. The lipid content did not change significantly ($P < 0.01$) in the first 4 days pi of the plant and ranged from 0.023 to 0.031 μg per nematode. From 6 days pi onwards, the lipid content increased significantly until the formation of mature females (15 days pi) and ranged from 0.153 to 21.029 μg per nematode (Fig. 2, Table 1). Since *C. elegans sbp-1* is involved in lipid metabolism, we speculated a similar role for *Mi-sbp-1* in the *M. incognita* life cycle and determined the developmental stage-specific expression of *Mi-sbp-1*. Compared with the egg stage, *Mi-sbp-1* was significantly ($P < 0.05$) down-regulated in the pre-parasitic J2s, post-parasitic J2s and mature females (MF), but was up-regulated in the J3s, J4s and young females (YF) (Fig. 3).

3.3. RNA-Seq of sbp-1 silenced nematode J2s

Total RNA from dsRNA-soaked (FD), starved (ST) and fresh (FR) *M. incognita* J2s was extracted and sequenced using the Illumina HiSeq platform in paired-end format. Two replicates were used for each treatment condition. The raw and quality-filtered data statistics for the sequenced samples used in this study are provided in Supplementary Table S2, and the raw data has been deposited to the Sequence Read Archives (Bioproject: PRJNA482752; biosample: SAMN09711864; sample accession numbers: SRR7601328 to SRR7601333). We obtained 30.59 to 40.07 million raw reads for each of the samples. A stringent criterion of 70:20 was used to obtain high quality filtered reads wherein >70% high quality (HQ) bases, each having Phred scores >20, were considered for further analyses. After quality filtering with the NGS QC tool, 30.18 to 39.67 million HQ reads were obtained (Supplementary Table S2). The HQ reads were 98.63% to 99.18% of the total raw reads with an average read length of 101 bp and were used for further downstream analyses.

A rapid method was used to interpret significant biology from the raw transcriptomic sequence data (Fig. 4A). The Transcripts Per Kilobase Million (TPM) values were used to discern replicate correlation by Principal Component Analysis (PCA). The PCA plot suggested a strong correlation between the biological replicates from the FD, ST and FR samples as the biological replicates clustered together with the other replicates of the respective treatments (Fig. 4B). The HQ reads from each of the replicates were mapped to the pre-annotated *M. incognita* proteome, and the annotation was directly used to interpret the results of our RNA-Seq data, thereby avoiding the need to assemble the transcriptomic sequences again. The read alignment of RNA-Seq samples used in this study showed that 51.82–82.59% HQ reads mapped to the

A.

>Minc3s00144g05954

MAQPSYFYSSPSSGCSAGTLLSPLSNGGVCSYPSVATSDFLEESDSQIDQDYWGEGEMAEGAEINSTAYKNDQLA
RGSEEGNTGHRERQGRRKSHKTERRTAHNLIEKKYRCSINDRINQLKEMLATEDNTKLSKSATLRRAVENIHSLR
SKNAELAGENGRLRRALEMAGLRDTGKIGGINKSSTMIVGQHTEQPEILLKGPNMQRSRISSSIKKCNNNNTSIS
STNVPSVVGPRDQSRVTLCVFMFLLLIYNPLAFLFTENSTNSSTFGADLQENTAIFGRHRTLTGDDFFVKDNTNK
IPFTSQSYVSVNSFEHWPNSSLLRHSLIWLLNCLFVFAILNRLLVSGEPVADRRSPRWGTFIQSRRKAQQAVAAG
NWKEAQRCLGESLQILERPLPSSGGLDEWMSLIWQIIRHLLNVLWIGRWFARRRRSSLQTQKSVCRSHAATSMVY
NQLHQLHLLGVDGIGLTQRGALNIALLAANLAESAGSSAISHALRAEMYACAAIRCRLCLPRWLRLPIAGYFFRR
AKRHVSKSHRLEGNAEQIYSLQWAFHPLARKFLADPLRLAAILDGSGAQRQTNFPFTDSTQSAKPLEVLRDAFKI
HLLDALITQIDSSEGLRVPDFVERSQLLLQICIANGNDTSVKCKETVGESSRTDGEALSDILLSSNSSAGDELCT
WWAHLLSSALHWRHGDMARARQHNAIVRKCPQNLLQSDTALAVGLAFCSRKICLEDRKQKAWKEIALLHVEKAFA
HLQRENRFHRWQVPLECQGQGIEKIHTGYIQEHEGITIMDQPEQKELQEKTFWQLSNNQQLGSVNDSPPPLPSIS
SKLPNKNNSLLNNEERTVKQELSATNTDEIQNYNNTGEAAILAKQEFLQLLLQITPEELEHLRARKALQAQSIQQ
PHNHQQFNYNNTTTIQSSQPIFIQTGQQQPQQLQYNQNPSIYTQQQQSSPPLDPLPPLVPYQIDYGITQSINTIN
NPMGHYGVQQVSETRKEI

Position 90 - 173 (bold red font); Helix-loop-helix DNA-binding domain superfamily (IPR036638)
Position 98 - 266, 322 - 460 (blue shaded); PTHR12565 (sterol regulatory element-binding protein domain)

B.

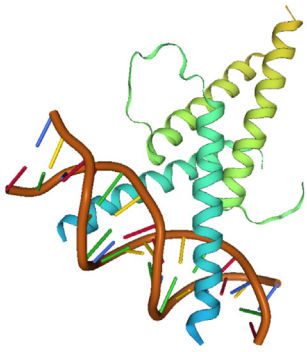

Predicted secondary structure model of Minc3s00144g05954

C.

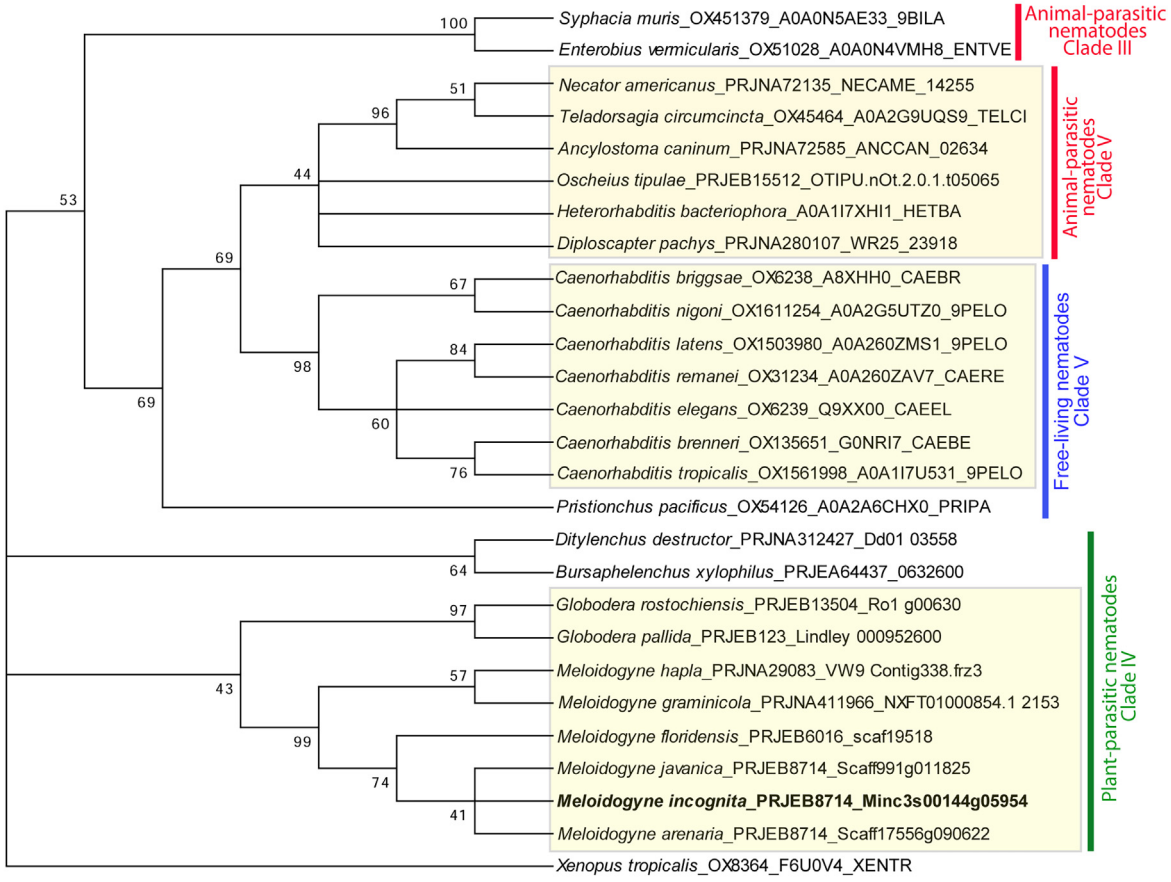

Fig. 1. Characterization of the translated sequence of the *Meloidogyne incognita* sterol-binding protein Mi-SBP-1 (Minc3s00144g05954). (A) The amino acid sequence shows the presence of a helix-loop-helix DNA binding domain (IPR036638, bold red (bold) font) and sterol regulatory element binding domain (PTHR12565, blue shaded (non-bold, shaded)). (B) The secondary structure prediction of the Minc3s00144g05954 transcript at https://swissmodel.expasy.org matched it to a helix-loop-helix containing DNA binding microphthalmia-associated transcription factor template 4atk.1; brown colour represents DNA strands; blue-green-yellow shaded ribbons represent amino acids. (C) The maximum likelihood phylogenetic analysis of SBP-1 protein sequences based on the JTT (Jones-Taylor-Thornton) matrix-based model grouped Minc3s00144g05954 with SBP-1 sequences of other *Meloidogyne* spp. The tree was bootstrapped 1000 times (values indicated at nodes), and the partitions reproduced in less than 40% bootstrap replicates were collapsed. The sequence name lists the nematode species, genome project accession number and SBP-1 sequence accession number. *Xenopus tropicalis* SBP-1 sequence was used as an out-group. Yellow shaded boxes represent the clades resolved in our analysis. The phylogenetic tree was generated using MEGA6.

already annotated *M. incognita* proteome, representing 80.51–82.90% of the total predicted 43,719 transcripts (Supplementary Table S3).

The effect of *Mi-sbp-1* silencing on the transcriptome of *M. incognita* was elucidated by comparing the transcripts of dsRNA-soaked (FD) and starved (ST) nematodes with the fresh juvenile control (FR). Compared with FR J2s, 579 transcripts were down-regulated, and 93 transcripts were up-regulated in FD J2s, whereas in ST J2s, 530 transcripts were down-regulated and 462 were up-regulated (Fig. 4C; Supplementary Data S1). Compared with FR controls, the number of unique down-regulated transcripts in FD and ST treatments were 368 and 319, respectively, whereas 39

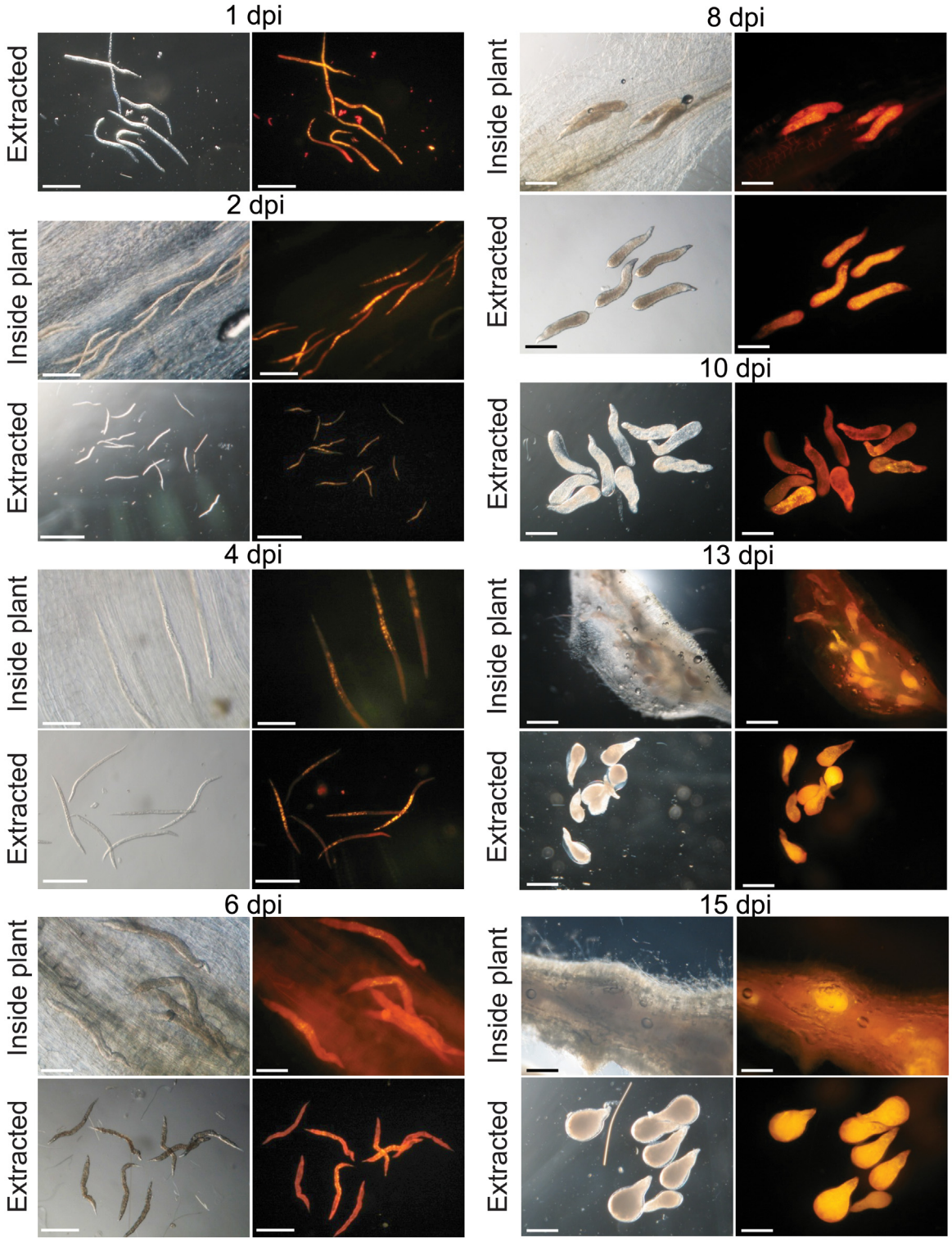

Fig. 2. Visualization of lipid content during different developmental stages of *Meloidogyne incognita*. The nematodes were allowed to grow on adzuki plant roots, and the lipid content was observed at 1, 2, 4, 6, 8, 10, 13 and 15 days p.i. (dpi) after Nile Red staining. (Extracted: nematodes dissected out from the plant roots; inside plants: nematodes feeding within the plant tissue).

and 408 unique transcripts were up-regulated in FD and ST treatments, respectively (Fig. 4C). The DEGs were subjected to a GO-Elite pathway analysis to find out the most significant pathways operating in FD and ST treatments. A complete list of pathways with a number of active transcripts is provided in Supplementary Data S1. The top five pathways active in FD J2s compared with FR (control) J2s were adenyl ribonucleotide binding (GO:0032559), protein catabolic process (GO:0030163), body morphogenesis (GO:0010171), zinc ion binding (GO:0008270) and proteolysis (GO:0006508). On the other hand, the top five pathways active in ST J2s compared with the controls were oxidation–reduction process (GO:0055114), proteolysis (GO:0006508), extracellu-

Table 1
The growth parameters and lipid reserves at different life stages of *Meloidogyne incognita* extracted from adzuki plants at different days post inoculation (mean ± S.E.M.). At least 30 specimens were measured for each incubation period.

Days p.i.	Body length (μm)	Greatest body width (μm)	Body mass (μg)	Lipid stained area (%)	Lipid content (μg)
0	329.5 ± 9.19[a]	13.3 ± 0.14[a]	0.036[a]	63.6 ± 7.2[a]	0.023[a]
1	313 ± 11.31[a]	14.1 ± 0.28[a]	0.039[a]	60.12 ± 6.66[a]	0.024[a]
2	354.5 ± 23.33[b]	14.75 ± 0.21[a]	0.048[ab]	46.22 ± 3.39[b]	0.023[a]
4	427 ± 16.97[c]	16.95 ± 0.21[b]	0.077[c]	39.34 ± 4.21[b]	0.031[a]
6	473.5 ± 19.09[d]	30.6 ± 0.82[c]	0.277[d]	53.31 ± 6.22[c]	0.153[b]
8	485 ± 8.49[d]	64.7 ± 1.09[d]	1.269[e]	55.12 ± 4.32[c]	0.723[c]
10	463 ± 8.49[d]	73.8 ± 1.11[e]	1.576[e]	61.23 ± 3.34[d]	0.997[d]
13	519 ± 9.90[e]	288 ± 16.66[f]	26.90[f]	79.32 ± 4.20[e]	22.050[e]
15	515.5 ± 9.19[e]	274 ± 21.24[f]	24.18[f]	84.16 ± 5.1[e]	21.029[e]

[a,b,c,d,e,f] Statistically significant differences at $P < 0.01$, Tukey's Honestly Significant Difference (HSD) test. The same letters indicate the same statistical groups.

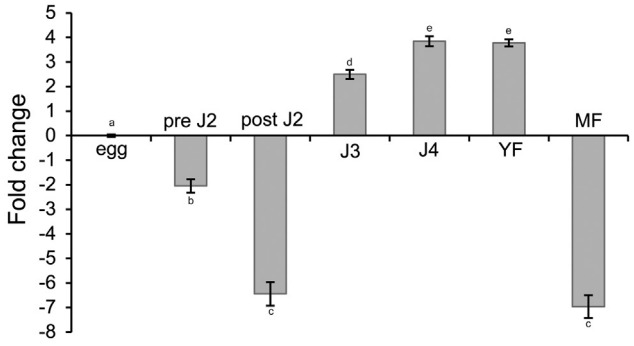

Fig. 3. Expression of *Mi-sbp-1* at different developmental stages of *Meloidogyne incognita*. Fold-change expression of the *Mi-sbp-1* gene in the different developmental stages of *M. incognita* compared with the egg stage. [a,b,c,d,e]Satistically significant differences at $P < 0.01$. J2, second stage juvenile; J3, third stage juvenile; J4, fourth stage juvenile; YF, young female; MF, mature female; pre J2, pre-parasitic J2; post J2, pos-tparasitic J2.

lar region (GO:0005576), carbohydrate metabolic process (GO:0005975) and intrinsic to plasma membrane (GO:0031226).

The carbon and fat metabolism pathways were specifically compared between FD and ST samples, and the expression of a few of the transcripts belonging to both pathways was validated by qRT-PCR. The qRT-PCR results confirmed the expression patterns of transcripts as obtained by RNA-Seq (Supplementary Data S1). Comparison of the transcripts in FD and ST samples is represented in Supplementary Data S1 and Supplementary Fig. S2. A total of 14 transcripts active in carbon pathways were identified (Supplementary Fig. S2A). A few noteworthy transcripts that showed down-regulation in FD nematodes compared with the ST nematodes were glyceraldehyde-3-phosphate dehydrogenase 2, fructose-bisphosphate aldolase 1, glycine cleavage system P protein, phosphotransferase and isocitrate dehydrogenase (NADP). Three transcripts annotated as glycine cleavage system P protein remained up-regulated.

In the fat metabolism pathway, 38 transcripts were identified, and a comparison of their expression between FD and ST samples is presented in Supplementary Fig. S2B. The three transcripts of *Mi-sbp-1* (Minc3s00144g05954, Minc3s00956g19271 and Minc3s00956g19270) showed significant up-regulation in the starved (ST) samples but were down-regulated in the silenced (FD) samples. The notable transcripts showing up-regulation in the unsilenced starved (ST) J2s but down-regulation or baseline expression in silenced (FD) J2s were 3-hydroxyacyl-CoA dehydrogenase, adipose triglyceride lipase, *fat-5*, *fat-4*, *elo-2*, sphingomyelin phosphodiesterase 1, glutaryl-CoA dehydrogenase, isovaleryl-CoA dehydrogenase, two phospholipases of patatin family, glucosylceramidase 3, and phospholipase B-like 1. There were a few transcripts that were down-regulated in starved (ST), but showed baseline expression in silenced (FD) J2s, such as four cytochrome P450s, *pod-2*, leukotriene A4 hydrolase, glucosylceramidase 3 and aminopeptidase-1. Thirteen transcripts that were down-regulated in both the silenced (FD) and starved (ST) samples were two cytochrome P450s, galactosidase/N-acetylgalactosamini dase, hypothetical protein with a phospholipase A2 domain, three low-density lipoprotein receptor-related protein (*lrp*), two lipases, one hypothetical protein belonging to short-chain dehydrogenase/reductase family, *let-767*, and aminopeptidase-1. Only one transcript, Minc3s01159g21258, encoding for *fat-7* was up-regulated in both sample types (FD and ST). These results suggest that *Mi-sbp-1* actively regulates the expression of lipogenesis as well as some amino acid metabolism genes in *M. incognita*.

3.4. Mi-sbp-1 expression and nematode stored fat profile

The fat content of *M. incognita* J2s declined steadily after starvation at 28 °C (Fig. 5A). The freshly hatched J2s contained ~0.025 μg of lipids, whereas upon starvation the lipid content started decreasing after 4 days (~0.021 μg), and decreased to ~0.008 μg after 10 days of starvation (Supplementary Table S4). However, the nematode body mass remained constant in the fresh and 10 days starved J2s (Fig. 5A). The expression of *Mi-sbp-1* was analysed in starved J2s at different time intervals by qRT-PCR. Compared with fresh J2s, the expression of *Mi-sbp-1* increased significantly ($P < 0.05$) upon starvation from 0.7 fold at 2 days to 4.75 fold at 10 days (Fig. 5B). In addition, the plant parasitism by 2, 4, 6, 8 and 10 days starved J2s was significantly ($P < 0.05$) reduced in eggplant compared with freshly hatched J2s, as measured by a nematode multiplication factor of 253.9 in freshly hatched J2s compared with 16 in 10 days starved J2s (Supplementary Table S5).

To evaluate the effect of silencing of *Mi-sbp-1* on nematode fat content, the freshly hatched nematode J2s were soaked in *Mi-sbp-1* dsRNA for 48 h, starved at 28 °C for 6 days, and stained with Nile Red. After 6 days of starvation, the *Mi-sbp-1* dsRNA soaked J2s showed significantly ($P < 0.05$) more body lipid content (~0.022 μg) compared with control starved J2s (~0.017 μg) (Fig. 5C, Supplementary Table S6). *Mi-sbp-1* silencing caused a three-fold significant ($P < 0.05$) reduction in the expression of *Mi-sbp-1* compared with the dsGFP control (Fig. 5D).

3.5. Effect of Mi-sbp-1 silencing on invasion, development and reproduction of M. incognita

In order to evaluate the effect of *Mi-sbp-1* silencing on nematode development and reproduction, an infection bioassay was conducted on adzuki bean plants using germination pouches. At 30 days pi, adzuki plants infected with *Mi-sbp-1* dsRNA-soaked worms showed a significant ($P < 0.05$) reduction in parasitism

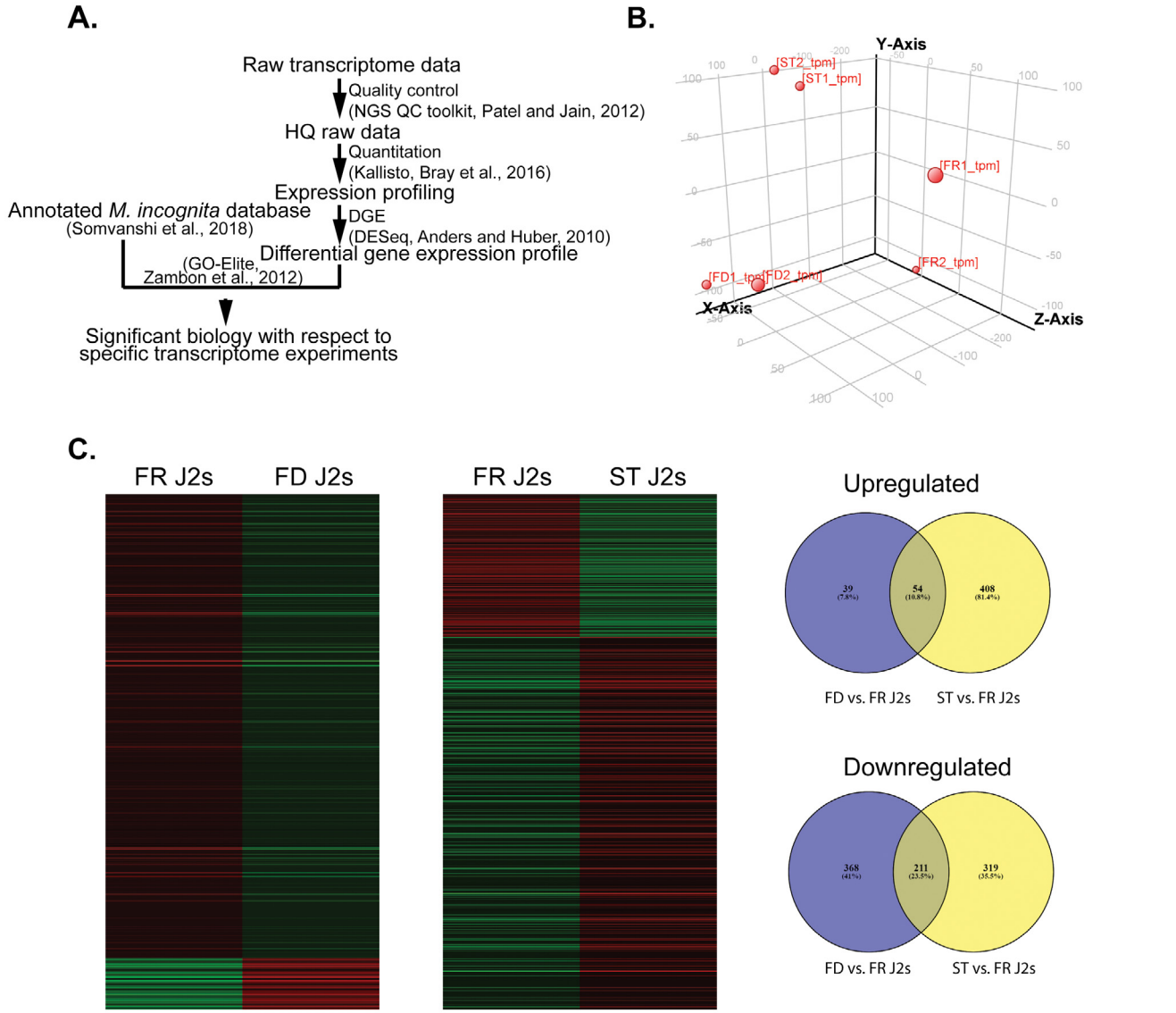

Fig. 4. RNA-Seq experiment to determine transcriptomic changes in *Mi-sbp-1* silenced *Meloidogyne incognita* J2s. (A) Methodology for a novel and faster approach to annotate the differentially expressed genes from the RNA-Seq experiment. (B) The replicate correlation by the Principal Component Analysis. (C) The representation of the differentially expressed transcripts as a heat map, and the upregulated and downregulated genes by Venn diagram. FR, fresh juvenile control; FD, double-stranded (ds)RNA-soaked nematodes; ST, starved nematodes.

and delayed development compared with the control (Fig. 6A). It was found that the growth and development of *Mi-sbp-1* dsRNA-soaked J2s were significantly ($P < 0.05$) slower compared with the control J2s. The silenced J2s took 6 and 8 days to reach the J4 and YF stage, respectively, compared with 4 and 5 days taken by the control J2s (Supplementary Table S7). *Mi-sbp-1* silenced nematodes exhibited delayed reproduction in terms of a reduced number of galls and egg masses per plant, eggs per egg mass and the multiplication factor (Fig. 6B). The multiplication factor, indicative of reproductive fitness and parasitic success, was reduced to 198 ± 56 in plants infected with *Mi-sbp-1* dsRNA-soaked J2s compared with controls (385 ± 40). In summary, silencing of *Mi-sbp-1* in pre-parasitic J2s caused delayed development and significant reduction in root galling and the multiplication factor.

3.6. Effect of transgenic tobacco plant expressing Mi-sbp-1 dsRNA on nematode biology

Agrobacterium tumefaciens (LBA4404) harbouring the hairpin gene construct of *Mi-sbp-1* as well as an empty control vector were used for co-cultivation of tobacco leaf disks. Preliminary screening by kanamycin selection and regeneration resulted in the identification of five primary *Mi-sbp-1* dsRNA transgenic events (T_0), which were confirmed by molecular analysis of each event by PCR using gene-specific sense, antisense, and *nptII* selectable markers. No significant phenotypic difference in the untransformed control plant grown on non-selective medium and T_0 plants grown on selective medium was observed (data not shown), indicating that neither the selectable marker nor the host-induced gene silencing (HIGS) affected the growth of transgenic plants. The T_1 progeny plants were generated by screening the seeds of T_0 plants in the presence of the antibiotic kanamycin. The progeny were re-validated by PCR using a gene-specific sense, antisense and *nptII* selectable marker, indicating stable integration and inheritance of the *Mi-sbp-1* dsRNA construct in the progeny plants (Supplementary Fig. S3). The qRT-PCR assay indicated significant expression of *Mi-sbp-1* dsRNA in all the selected T_1 events, whereas no transcript was detected in untransformed control tobacco plants (Supplementary Fig. S4). The expression data of *Mi-sbp-1* for the transformed lines is presented (as 1 Ct) relative to the 18S RNA gene and significantly

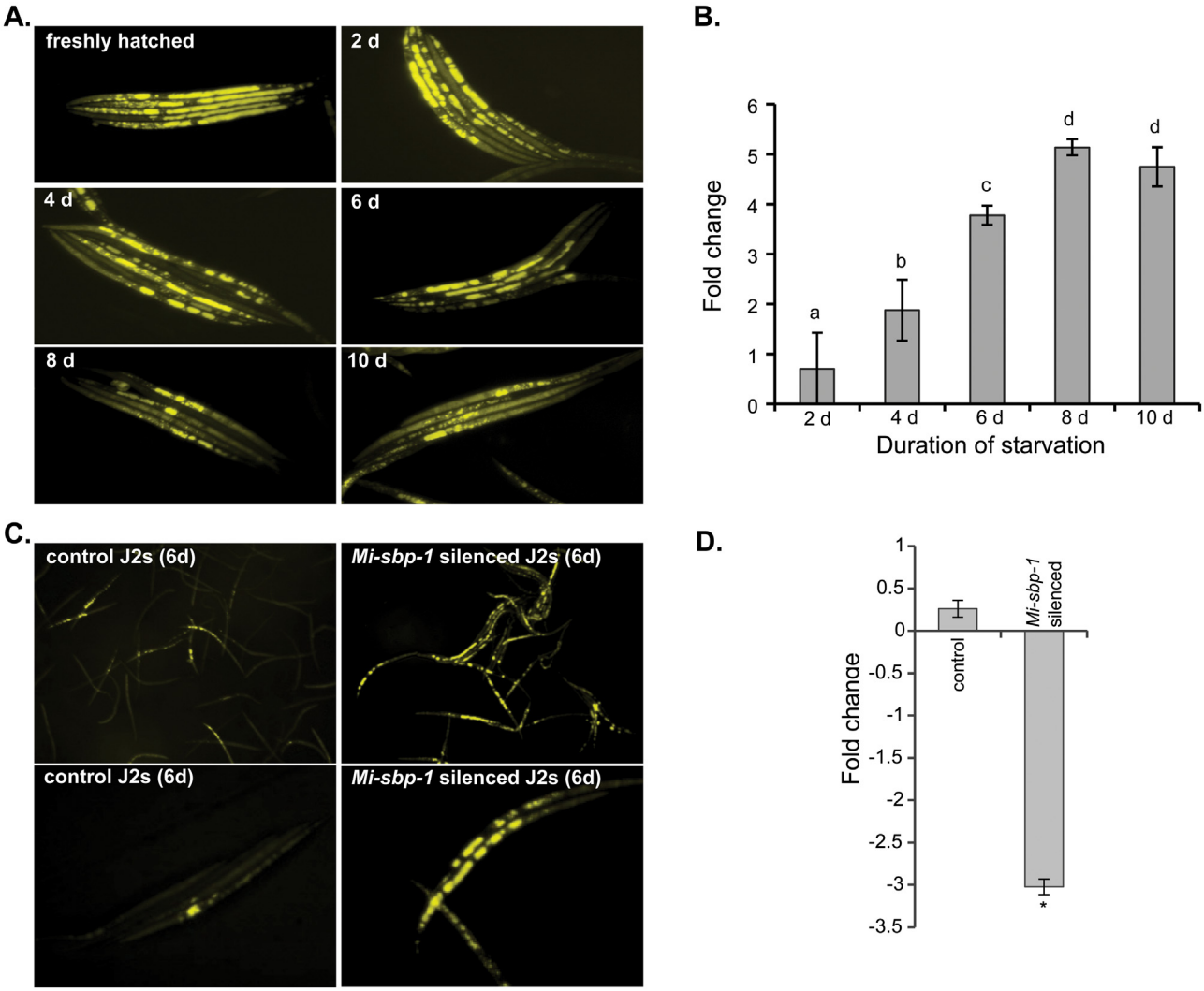

Fig. 5. Correlation between lipid content of *Meloidogyne incognita* J2s and expression of *Mi-sbp-1*. (A) Nile Red staining of *M. incognita* J2s showing variation in lipid content in the freshly hatched J2s and J2s starved for 2, 4, 6, 8 and 10 days (d) at 28 °C. (B) Fold change expression of the *Mi-sbp-1* gene at different starvation periods compared with freshly hatched J2s. (C) Lipid content of 6 days starved control and *Mi-sbp-1* silenced J2s. (D) Expression of the *Mi-sbp-1* gene in control and *Mi-sbp-1* silenced J2s.

($P < 0.05$) greater expression of *Mi-sbp-1* dsRNA was documented for all the events (Supplementary Fig. S5A). The effectiveness of HIGS on the *Mi-sbp-1* transcript in nematodes was determined by qRT-PCR in *M. incognita* females extracted from the T_1 transgenic tobacco plants at 20 days pi. Results showed that *Mi-sbp-1* was significantly ($P < 0.05$) down-regulated to −1.34 fold compared with control female nematodes (Supplementary Fig. S5B).

The T_1 tobacco plants expressing *Mi-sbp-1* dsRNA were evaluated for nematode invasion, development and reproduction (Fig. 7A). At 30 days pi, T_1 tobacco plants showed considerably reduced numbers of galls with robust root systems compared with wild type plants. The number of galls per plant was significantly ($P < 0.05$) reduced by 31–42% compared with wild type plants. Additionally, 30–43.8% reduction in the number of egg masses was recorded in all the transgenic events compared with wild type controls. The females and egg masses extracted from the 13–5-7 T_1 event were found to be of smaller size (width 578 μm, length 768 μm) when compared with the control females (width 663 μm, length 943 μm) and egg masses extracted from wild type tobacco plants (Fig. 7B). The fecundity of *M. incognita* in terms of the number of eggs per egg mass was substantially decreased by 33–54% in *Mi-sbp-1* silenced transgenic lines compared with the wild type plants and finally the derived multiplication factor was significantly ($P < 0.05$) decreased by 46–66% in *Mi-sbp-1* silenced transgenic lines compared with the wild type plants (Fig. 7C, Supplementary Table S8).

4. Discussion

The mammalian sterol regulatory element-binding proteins (SREBPs) regulate lipid homeostasis by controlling the expression of enzymes required for endogenous cholesterol, fatty acid, triacylglycerol and phospholipid synthesis (Eberle et al., 2004). The three known isoforms of SREBP, viz., SREBP-1a, SREBP-1c and SREBP-2 perform different roles in lipid synthesis. SREBP1a is involved in lipid synthesis and growth, SREBP1c in fatty acid synthesis and energy storage, whereas SREBP2 is involved in cholesterol regulation (Shimano and Sato, 2017). The SREBP-1a and SREBP-2 isoforms are regulated by cellular sterol levels, whereas the SREBP-1c isoform is transcriptionally regulated by insulin (Eberle et al., 2004). SREBP-1c was suggested to be a potential therapeutic target for obesity and associated diseases in mammals due to its important role in fat metabolism (Nomura et al., 2010; Song and Xiao, 2013). *Caenorhabditis elegans* SBP-1. a homolog of mammalian

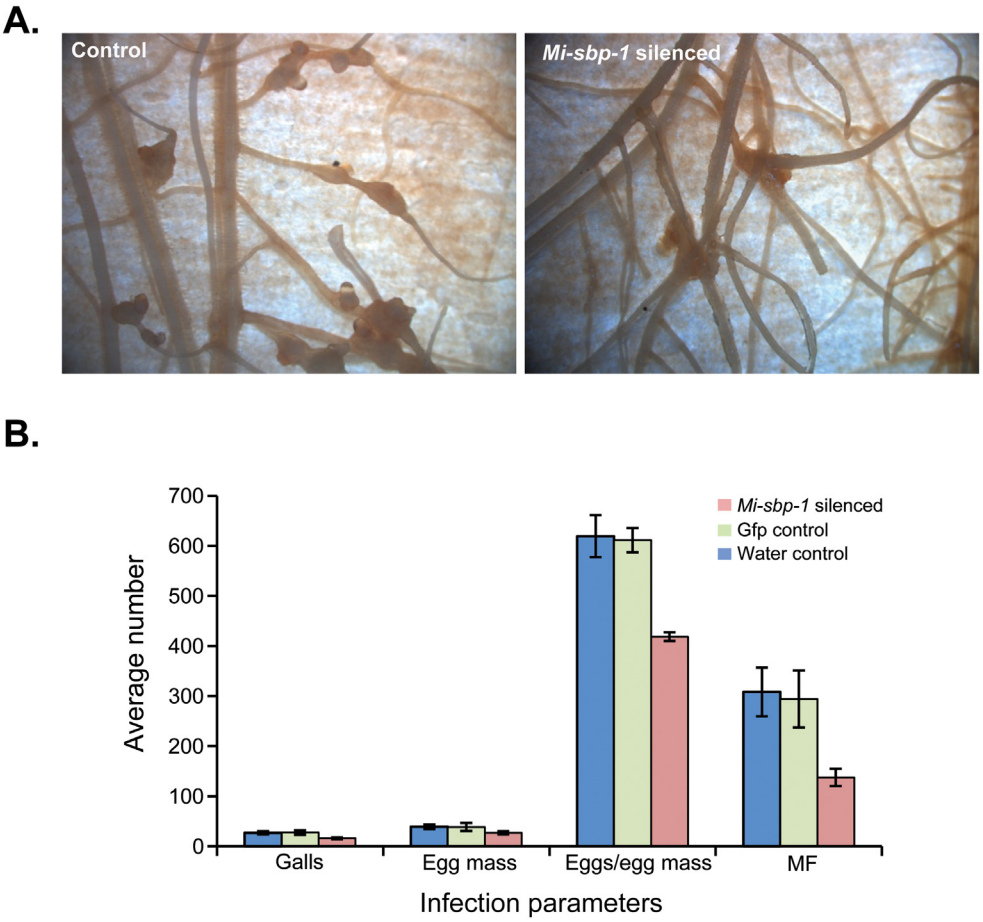

Fig. 6. Pathogenicity of *Meloidogyne incognita* J2s on adzuki plants upon silencing of *Mi-sbp-1*. (A) Galling in plant roots infected by control nematodes compared with *Mi-sbp-1* silenced nematodes. (B) Infection parameters of control and *Mi-sbp-1* silenced J2s on adzuki plants. Average number of galls, egg mass, eggs per egg mass and corresponding multiplication factor (MF) are represented. Columns represent the mean ± S.E. (n = 6).

SREBP-1c, expresses highly in the worm intestines (Nomura et al., 2010), and regulates expression of several genes of the lipogenesis pathway such as *pod-2*, *fasn-1*, glycerol 3-phosphate acyltransferase (GPAT), *elo-2*, *elo*-5, *elo-6*, *fat-2*, *fat-5*, *fat-6* and *fat-7* as well as starvation-inducible gene *acs-2* (Ashrafi et al., 2003; Kniazeva et al., 2003; McKay et al., 2003; Kniazeva et al., 2004; Nomura et al., 2010; Srinivasan, 2015; Watts and Ristow, 2017). Silencing of *sbp-1* in *C. elegans* caused a reduction in nematode body size, fat storage and egg laying activity (Nomura et al., 2010), whereas mutants defective in fat synthesis genes including *sbp-1*either showed developmental arrest of larvae or satiety quiescence (McKay et al., 2003; Hyun et al., 2016).

Despite advancements in the understanding of the biological role of SBP-1 in *C. elegans* biology and lipogenesis, its function in PPNs is largely unknown. In the present study, we identified a *C. elegans* SBP-1 homologue in an important PPN species, *M. incognita*. To the best of our knowledge, this is the first evidence for the functional role of a SREBP (Mi-SBP-1) in the development, reproduction and parasitism of an obligate root parasite of plants. The re-sequenced *Mi-sbp-1* (2159 bp) transcript was 100% identical to the cDNA Minc3s00144g05954 from the *M. incognita* genomic database (Abad et al., 2008), that encodes a basic helix-loop-helix (HLH) transcription factor homologous to the mammalian SREBP-1c (Eberle et al., 2004). The Southern blot hybridisation assay revealed that *Mi-sbp-1* is present in three copies in the *M. incognita* genome, where three analogues (Minc3s00144g05954, Minc3s00956g19271 and Minc3s00956g19270) for *Mi-sbp-1* are also known to be present (Abad et al., 2008). We found that silencing of *Mi-sbp-1* caused a significant down-regulation of several transcripts involved in lipogenesis, suggesting the role of *Mi-sbp-1* in regulating lipid metabolism gene expression in *M. incognita*.

Developmental stage-specific expression of *Mi-sbp-1* showed that it was down-regulated in the pre-parasitic J2s, post-parasitic J2s and mature females (MF) but up-regulated in the J3s, J4s and young females (YF). The pre- and post-parasitic J2s and females are the feeding stages, whereas J3s and J4s are non-feeding stages of the nematode species. The down-regulation of *Mi-sbp-1* in all feeding stages except YF indicates a lack of de novo lipogenesis in these stages. It is well-known that the soil-inhabiting pre-parasitic J2s rely on their stored lipid reserves for energy (Krusberg et al., 1973; da Silva Rocha et al., 2015), and during the sedentary endoparasitic phase, nematode development is dependent on feeding site formation inside the plant roots for a continuous food supply (Golinowski et al., 1999; Vanholme et al., 2004; Hofmann and Grundler, 2007; Hofmann et al., 2010). The down-regulated expression of *Mi-sbp-1* in pre- and post-parasitic J2s probably confirms that de novo lipid synthesis does not occur in J2s and they obtain their energy from the fat reserves. The same might be true for the mature female stage which lays eggs and requires energy and lipids. On the other hand, the non-feeding stages showing up-regulation of *Mi-sbp-1* indicates increased de novo lipogenesis (Chitwood and Perry, 2009). We also observed that upon starvation, the neutral lipid content in *M. incognita* J2s decreased over time, whereas the corresponding expression of

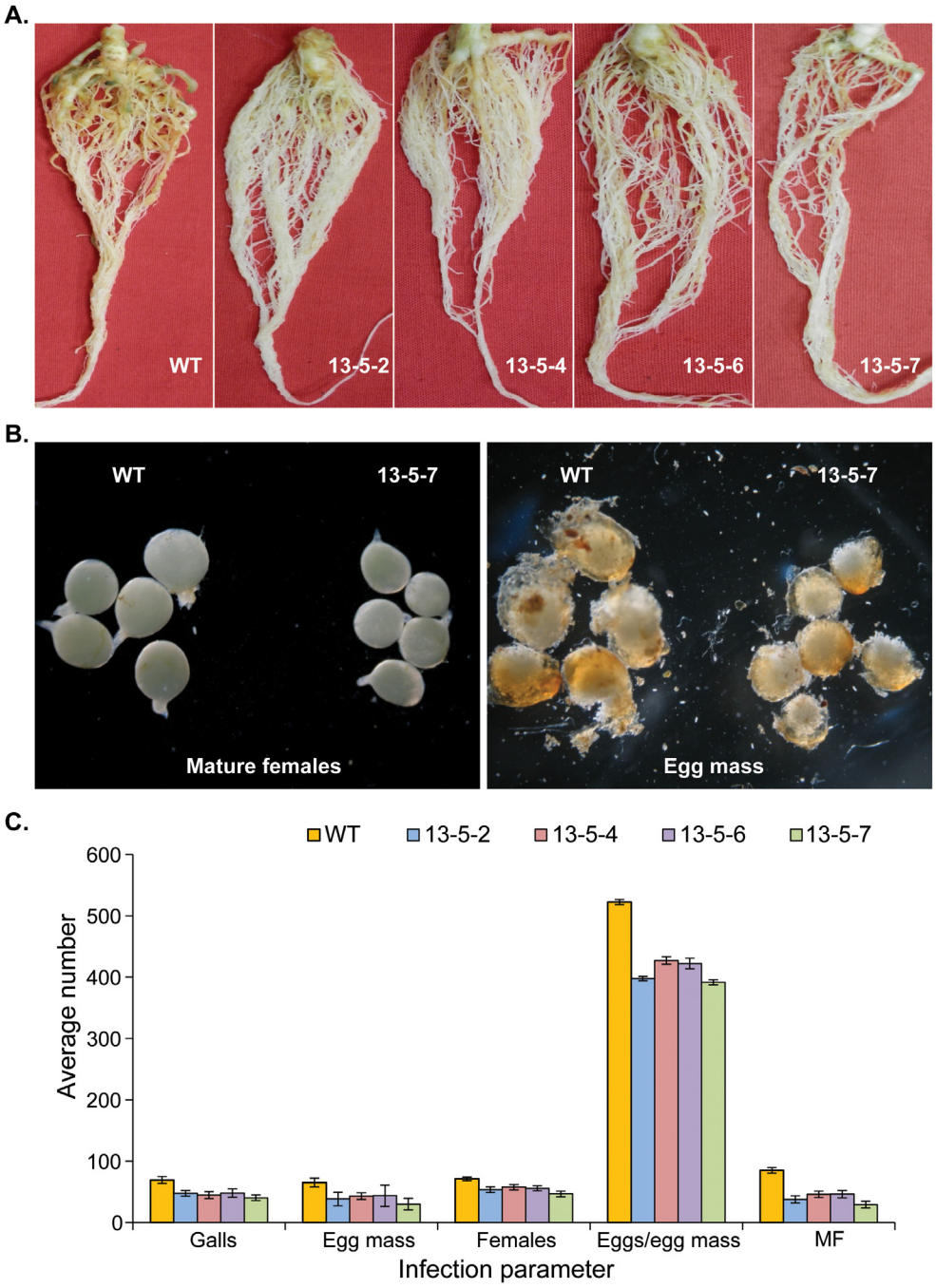

Fig. 7. Development and reproduction of *Meloidogyne incognita* on *Mi-sbp-1* double-stranded (ds)RNA expressing transgenic T1 tobacco plants. (A) Root volume and galling intensity of roots of wild type (WT) and *Mi-sbp-1* dsRNA expressing transgenic tobacco plants at 30 days p.i. (B) Comparative size of *M. incognita* females and egg masses from WT plants compared with transgenic plants. Adult females from T_1 plants of event 13-5-7 were smaller (length: 768.4 ± 58.29 μm; width: 578 ± 37.98) compared with the control (length: 943.5 ± 58.82 μm; width: 663 ± 68.57). Adult females from T_1 plant 13-5-7 produced smaller egg masses compared with those from control plants. (C) Effect of host delivered RNA interference (RNAi) events of *Mi-sbp-1* in T1 tobacco plants on development and reproduction of *M. incognita*. Average numbers of galls, egg masses, egg/egg mass and a corresponding multiplication factor (MF) of *M. incognita* in T_1 generation and WT tobacco plants at 30 days p.i. are represented. Each bar represents the mean ± S.E. (n = 8).

Mi-sbp-1 showed an up-regulation compared with fresh unstarved J2s (at day 0). The *Mi-sbp-1* up-regulation in J2s with time might appear contradictory to its expression profile in different life stages where it was found down-regulated in J2s. It is important to note that the developmental stage-specific expression of *Mi-sbp-1* was calculated using the egg stage as the reference, whereas here, the fresh unstarved J2s at 0 h are used for comparison to show relative expression upon starvation.

Another pertinent observation was that silencing of *Mi-sbp-1* in the J2s resulted in non-utilization of fat reserves, even after starvation, suggesting a connection between *Mi-sbp-1* and starvation-induced catabolism of stored fat in *M. incognita*, possibly through Delta (9)-fatty-acid desaturase (*fat-7*), also known as stearoyl-CoA desaturases. The expression of *fat-7* is negatively correlated to β-oxidation, and under fasting conditions, stored fat utilization through β-oxidation happens following a decrease in expression of *fat-7* and an increase in expression of *acs-2* (Van Gilst et al., 2005a, 2005b). Silencing of *sbp-1* in *C. elegans* caused a down-regulation of *elo-2*, *fat-2*, *fat-5*, *fat-6*, and *fat-7*. In our study, the *fat-7* gene was up-regulated in starved J2s and was at baseline in

the *Mi-sbp-1* silenced J2s (Supplementary Data S1). The expression of *fat-5*, *fat-6*, and *fat-7* is also controlled by other transcription factors such as *nhr-49* and *nhr-80* (Van Gilst et al., 2005a, 2005b; Brock and Watts, 2006). Both *sbp-1* and *nhr-49* are regulated by the same co-activator (*mdt-15*) (Taubert et al., 2006; Yang et al., 2006). Up-regulation of *fat-7* in *M. incognita* J2s might indicate a mechanism to slow down the exhaustion of stored fat in the J2 stage, as this stage has to survive in soil until a host is found. However, despite this suppression of β-oxidation, the stored fat levels dropped as time passed, which could have been facilitated by independent regulation of β-oxidation pathway genes by other regulatory genes as stated above. On the other hand, the slow utilisation of stored fat in *Mi-sbp-1* silenced J2s even after starvation could be happening through a *fat-7* based mechanism, which at baseline expression level might be causing a low-level suppression of β-oxidation, thus reducing the utilisation of fat reserves. The silencing of *Mi-sbp-1* also led to the down-regulation or baseline expression of several enzymes involved in fat catabolism, i.e., 3-hydroxyacyl-CoA dehydrogenase, adipose triglyceride lipase (*atgl-1*), several phospholipases belonging to the patatin family, phospholipase B-like 1 and lipid hydrolases, which might also contribute to the slow utilization of stored fat in the *Mi-sbp-1* silenced J2s. Additionally, lipolysis is also tightly linked to the expression of HLH domain-containing transcription factors (O'Rourke and Ruvkun, 2013), which could be involved in the fatty acid oxidation in yet unknown ways.

The in vitro and HIGS-mediated RNAi silencing of *Mi-sbp-1* reduced the parasitic potential, fecundity and multiplication factor (an indicator of reproductive fitness) of *M. incognita*. *Mi-sbp-1* silenced J2s were slower in development, less parasitic, and produced fewer eggs per egg mass on adzuki bean plants compared with the un-silenced J2s. The transgenic tobacco plants expressing the dsRNA of *Mi-sbp-1* caused a significant reduction in root penetration, development and fecundity of *M. incognita* compared with the wild type control. Also, *Mi-sbp-1* silencing caused aberrant phenotypes of *M. incognita* in relation to female size. Similar observations were recorded in *C. elegans* where the silencing of *sbp-1* caused a decrease in nematode body size and fat storage (Nomura et al., 2010). The decline in neutral lipid content was significantly correlated to the reduction in host-seeking behaviour and parasitic success of *M. incognita* in eggplant in an earlier study (da Silva Rocha et al., 2015).

In conclusion, our study demonstrates that *Mi-sbp-1* plays a key role in lipogenesis, biology and plant parasitism of the root-knot nematode, *M. incognita*. Unlike mammals with three SREBPs, *M. incognita* possessed only one *sbp-1* homolog regulating the expression of several downstream proteins and proved to be an effective choke point/target for its management, as disruption of *Mi-sbp-1* by RNAi resulted in a significant reduction in nematode parasitism and fecundity. To achieve higher nematode suppression than obtained by silencing *Mi-sbp-1* alone, multiple previously identified target genes could be disrupted in combination with *Mi-sbp-1*. Our study attempted to translate the existing basic knowledge of nematode fat metabolism from the model nematode *C. elegans* into a useful technology for the management of plant-parasitic root-knot nematodes, and sets an example for targeting nematode fat metabolism for the management of other parasitic nematodes.

Acknowledgements

Funding from the Department of Biotechnology, Government of India to UR through grant no. BT/PR5908/AGR/36/727/2012 "Translational research on root-knot nematode tolerant RNAi transgenics based on vital parasite gene targets from validation to proof-of-concept to selection of event(s) in the field under confined conditions" is acknowledged. The authors thank the Director and the Joint Director (Research), ICAR-Indian Agricultural Research Institute, New Delhi, India, for extending all the support and facilities to complete the study.

Appendix A. Supplementary data

Supplementary data to this article can be found online at https://doi.org/10.1016/j.ijpara.2019.09.002.

References

Abad, P., Gouzy, J., Aury, J.M., Castagnone-Sereno, P., Danchin, E.G., Deleury, E., Perfus-Barbeoch, L., Anthouard, V., Artiguenave, F., Blok, V.C., Caillaud, M.C., Coutinho, P.M., Dasilva, C., De Luca, F., Deau, F., Esquibet, M., Flutre, T., Goldstone, J.V., Hamamouch, N., Hewezi, T., Jaillon, O., Jubin, C., Leonetti, P., Magliano, M., Maier, T.R., Markov, G.V., McVeigh, P., Pesole, G., Poulain, J., Robinson-Rechavi, M., Sallet, E., Segurens, B., Steinbach, D., Tytgat, T., Ugarte, E., van Ghelder, C., Veronico, P., Baum, T.J., Blaxter, M., Bleve-Zacheo, T., Davis, E.L., Ewbank, J.J., Favery, B., Grenier, E., Henrissat, B., Jones, J.T., Laudet, V., Maule, A. G., Quesneville, H., Rosso, M.N., Schiex, T., Smant, G., Weissenbach, J., Wincker, P., 2008. Genome sequence of the metazoan plant-parasitic nematode *Meloidogyne incognita*. Nat. Biotechnol. 26, 909–915.

Abràmoff, M.D., Magalhães, P.J., Ram, S.J., 2004. Image processing with ImageJ. Biophotonics Int. 11, 36–42.

Andrassy, I., 1956. Die rauminhalts-und gewichtsbestimmung der fadenwürmer (Nematoden). Acta Zool. Hungarica 2, 1–5.

Ashrafi, K., Chang, F.Y., Watts, J.L., Fraser, A.G., Kamath, R.S., Ahringer, J., Ruvkun, G., 2003. Genome-wide RNAi analysis of *Caenorhabditis elegans* fat regulatory genes. Nature 421, 268–272.

Blaxter, M.L., De Ley, P., Garey, J.R., Liu, L.X., Scheldeman, P., Vierstraete, A., Vanfleteren, J.R., Mackey, L.Y., Dorris, M., Frisse, L.M., 1998. A molecular evolutionary framework for the phylum Nematoda. Nature 392, 71–75.

Branicky, R., Desjardins, D., Liu, J.L., Hekimi, S., 2010. Lipid transport and signaling in *Caenorhabditis elegans*. Dev. Dyn. 239, 1365–1377.

Bray, N.L., Pimentel, H., Melsted, P., Pachter, L., 2016. Near-optimal probabilistic RNA-seq quantification. Nat. Biotechnol. 34, 525–527.

Brock, T.J., Watts, J.L., 2006. Genetic regulation of unsaturated fatty acid composition in *C. elegans*. PLoS Genet. 2, e108.

Byrd, D.W., Kirkpatrick, T., Barker, K.R., 1983. An improved technique for clearing and staining plant tissues for detection of nematodes. J. Nematol. 15, 142–143.

Chirala, S.S., Wakil, S.J., 2004. Structure and function of animal fatty acid synthase. Lipids 39, 1045–1053.

Chitwood, D.J., Perry, R.N., 2009. Reproduction, physiology and biochemistry. In: Perry, R.N., Moens, M., Starr, J.L. (Eds.), Root-knot nematodes. CAB Int, Wallingford, UK, pp. 182–200.

Collange, B., Navarrete, M., Montfort, F., Mateille, T., Tavoillot, J., Martiny, B., Tchamitchian, M., 2014. Alternative cropping systems can have contrasting effects on various soil-borne diseases: Relevance of a systemic analysis in vegetable cropping systems. Crop Prot. 55, 7–15.

IHG Consortium, 2019. Comparative genomics of the major parasitic worms. Nat. Genet. 51, 163.

da Silva Rocha, F., Campos, V.P., Catão, H.C.R.M., Muniz, M.d.F.S., Civil, N., 2015. Correlations among methods to estimate lipid reserves of second-stage juveniles and its relationships with infectivity and reproduction of *Meloidogyne incognita*. Nematology 17, 345–352.

Danchin, E.G., Arguel, M.-J., Campan-Fournier, A., Perfus-Barbeoch, L., Magliano, M., Rosso, M.-N., Da Rocha, M., Da Silva, C., Nottet, N., Labadie, K., 2013. Identification of novel target genes for safer and more specific control of root-knot nematodes from a pan-genome mining. PLoS Pathog. 9, e1003745.

Eberle, D., Hegarty, B., Bossard, P., Ferre, P., Foufelle, F., 2004. SREBP transcription factors: master regulators of lipid homeostasis. Biochimie 86, 839–848.

Elling, A.A., 2013. Major emerging problems with minor *Meloidogyne* species. Phytopathology 103, 1092–1102.

Entchev, E.V., Schwudke, D., Zagoriy, V., Matyash, V., Bogdanova, A., Habermann, B., Zhu, L., Shevchenko, A., Kurzchalia, T.V., 2008. LET-767 is required for the production of branched chain and long chain fatty acids in *Caenorhabditis elegans*. J. Biol. Chem. 283, 17550–17560.

Faske, T., Hurd, K., 2015. Sensitivity of *Meloidogyne incognita* and *Rotylenchulus reniformis* to fluopyram. J. Nematol. 47, 316.

Foster, J.M., Zhang, Y., Kumar, S., Carlow, C.K., 2005. Mining nematode genome data for novel drug targets. Trend Parasitol. 21, 101–104.

Golinowski, W., Grundler, F., Sobczak, M., 1999. Ultrastructure of feeding plugs and feeding tubes formed by *Heterodera schachtii*. Nematology 1, 363–374.

Hofmann, J., El Ashry, A.E.N., Anwar, S., Erban, A., Kopka, J., Grundler, F., 2010. Metabolic profiling reveals local and systemic responses of host plants to nematode parasitism. Plant J. 62, 1058–1071.

Hofmann, J., Grundler, F., 2007. How do nematodes get their sweets? Solute supply to sedentary plant-parasitic nematodes. Nematology 9, 451–458.

Hughes, J.P., Rees, S., Kalindjian, S.B., Philpott, K.L., 2011. Principles of early drug discovery. Br. J. Pharmacol. 162, 1239–1249.

Hyun, M., Davis, K., Lee, I., Kim, J., Dumur, C., You, Y.-J., 2016. Fat metabolism regulates satiety behavior in *C. elegans*. Sci. Rep. 6, 24841.

Jones, J.T., Haegeman, A., Danchin, E.G., Gaur, H.S., Helder, J., Jones, M.G., Kikuchi, T., Manzanilla-López, R., Palomares-Rius, J.E., Wesemael, W.M., 2013. Top 10 plant-parasitic nematodes in molecular plant pathology. Mol. Plant Patho. 14, 946–961.

Kearn, J., Ludlow, E., Dillon, J., O'Connor, V., Holden-Dye, L., 2014. Fluensulfone is a nematicide with a mode of action distinct from anticholinesterases and macrocyclic lactones. Pest Biochem. Physiol. 109, 44–57.

Kim, K.-H., Kabir, E., Jahan, S.A., 2017. Exposure to pesticides and the associated human health effects. Sci. Total Environ. 575, 525–535.

Kniazeva, M., Crawford, Q.T., Seiber, M., Wang, C.Y., Han, M., 2004. Monomethyl branched-chain fatty acids play an essential role in *Caenorhabditis elegans* development. PLoS Biol. 2, e257.

Kniazeva, M., Sieber, M., McCauley, S., Zhang, K., Watts, J.L., Han, M., 2003. Suppression of the ELO-2 FA elongation activity results in alterations of the fatty acid composition and multiple physiological defects, including abnormal ultradian rhythms, in *Caenorhabditis elegans*. Genetics 163, 159–169.

Krusberg, L., Hussey, R., Fletcher, C., 1973. Lipid and fatty acid composition of females and eggs of *Meloidogyne incognita* and *M. arenaria*. Comp. Biochem. Physiol. B: Biochem. Mol. Biol. 45, 335–341.

Kumar, S., Chaudhary, K., Foster, J.M., Novelli, J.F., Zhang, Y., Wang, S., Spiro, D., Ghedin, E., Carlow, C.K., 2007. Mining predicted essential genes of *Brugia malayi* for nematode drug targets. PLoS ONE 2, e1189.

Kumar, S., Stecher, G., Tamura, K., 2016. MEGA7: molecular evolutionary genetics analysis version 7.0 for bigger datasets. Mol. Biol. Evol. 33, 1870–1874.

Kyndt, T., Vieira, P., Gheysen, G., de Almeida-Engler, J., 2013. Nematode feeding sites: unique organs in plant roots. Planta 238, 807–818.

Lahm, G.P., Desaeger, J., Smith, B.K., Pahutski, T.F., Rivera, M.A., Meloro, T., Kucharczyk, R., Lett, R.M., Daly, A., Smith, B.T., 2017. The discovery of fluazaindolizine: a new product for the control of plant parasitic nematodes. Bioorg. Med. Chem. Lett. 27, 1572–1575.

Lee, J.H., Kong, J., Jang, J.Y., Han, J.S., Ji, Y., Lee, J., Kim, J.B., 2014. Lipid droplet protein LID-1 mediates ATGL-1-dependent lipolysis during fasting in *Caenorhabditis elegans*. Mol. Cell. Biol. 34, 4165–4176.

Livak, K., Schmittgen, T., 2001. Analysis of relative gene expression data using real-time quantitative PCR and the 2-DDCT method. Methods 25, 402–408.

Love, M.I., Huber, W., Anders, S., 2014. Moderated estimation of fold change and dispersion for RNA-seq data with DESeq2. Genome Biol. 15, 550.

McKay, R.M., McKay, J.P., Avery, L., Graff, J.M., 2003. *C elegans*: a model for exploring the genetics of fat storage. Dev. Cell 4, 131–142.

Mitreva, M., Zarlenga, D.S., McCarter, J.P., Jasmer, D.P., 2007. Parasitic nematodes—from genomes to control. Vet. Parasitol. 148, 31–42.

Nicol, J., Turner, S., Coyne, D., Den Nijs, L., Hockland, S., Maafi, Z.T., 2011. Current nematode threats to world agriculture. In: Jones, J., Gheysen, G., Fenoll, C. (Eds.), Genomics and Molecular Genetics of Plant-Nematode Interactions. Springer, Berlin, Heidelberg, pp. 21–43.

Nomura, T., Horikawa, M., Shimamura, S., Hashimoto, T., Sakamoto, K., 2010. Fat accumulation in *Caenorhabditis elegans* is mediated by SREBP homolog SBP-1. Genes Nutr. 5, 17–27.

O'Rourke, E.J., Ruvkun, G., 2013. MXL-3 and HLH-30 transcriptionally link lipolysis and autophagy to nutrient availability. Nat. Cell Biol. 15, 668–676.

Papolu, P.K., Gantasala, N.P., Kamaraju, D., Banakar, P., Sreevathsa, R., Rao, U., 2013. Utility of host delivered RNAi of two FMRF amide like peptides, *flp-14* and *flp-18*, for the management of root knot nematode, *Meloidogyne incognita*. PLoS One 8, e80603.

Patel, R.K., Jain, M., 2012. NGS QC Toolkit: a toolkit for quality control of next generation sequencing data. PLoS ONE 7, e30619.

Phani, V., Somvanshi, V.S., Shukla, R.N., Davies, K.G., Rao, U., 2018. A transcriptomic snapshot of early molecular communication between Pasteuria penetrans and Meloidogyne incognita. BMC Genomics 19, 850.

Rappleye, C.A., Tagawa, A., Le Bot, N., Ahringer, J., Aroian, R.V., 2003. Involvement of fatty acid pathways and cortical interaction of the pronuclear complex in *Caenorhabditis elegans* embryonic polarity. BMC Dev. Biol. 3, 8.

Reddy, J.K., Hashimoto, T., 2001. Peroxisomal β-oxidation and peroxisome proliferator–activated receptor α: an adaptive metabolic system. Annu. Rev. Nutr. 21, 193–230.

Hussey, 1985. Host-parasite relationships and associated physiological changes. In: Sasser, J.N., Carter, C.C. (Eds.), An advanced treatise on *Meloidogyne*. Volume I: Biology and control. North Carolina State University, Raleigh, NC, pp. 143–153.

Shimano, H., Sato, R., 2017. SREBP-regulated lipid metabolism: convergent physiology — divergent pathophysiology. Nat. Rev. Endocrinol. 13, 710–730.

Shivakumara, T.N., Chaudhary, S., Kamaraju, D., Dutta, T.K., Papolu, P.K., Banakar, P., Sreevathsa, R., Singh, B., Manjaiah, K.M., Rao, U., 2017. Host-induced silencing of two pharyngeal gland genes conferred transcriptional alteration of cell wall-modifying enzymes of *Meloidogyne incognita* vis-à-vis perturbed nematode infectivity in eggplant. Front. Plant Sci. 8, 473.

Shivakumara, T.N., Dutta, T.K., Mandal, A., Rao, U., 2018. Estimation of lipid reserves in different life stages of *Meloidogyne incognita* using image analysis of Nile Red-stained nematodes. Nematology 21, 267–274.

Shivakumara, T.N., Papolu, P.K., Dutta, T.K., Kamaraju, D., Chaudhary, S., Rao, U., 2016. RNAi-induced silencing of an effector confers transcriptional oscillation in another group of effectors in the root-knot nematode, *Meloidogyne incognita*. Nematology 18, 857–870.

Slomczynska, U., South, M.S., Bunkers, G., Edgecomb, D., Wyse-Pester, D., Selness, S., Ding, Y., Christiansen, J., Ediger, K., Miller, W., 2014. Tioxazafen: A new broad-spectrum seed treatment nematicide. In: Maienfisch, P., Stevenson, T.M. (Eds.), ACS Symposium Series, Vol. 1204, Discovery and synthesis of crop protection products. Monsanto Corporation, Chesterfield, Missouri, pp. 129-147..

Somvanshi, V.S., Ghosh, O., Budhwar, R., Dubay, B., Shukla, R.N., Rao, U., 2018. A comprehensive annotation for the root-knot nematode *Meloidogyne incognita* proteome data. Data Brief 19, 1073–1079.

Song, B.-L., Xiao, X., 2013. SREBP: a novel therapeutic target. Acta Biochim. Biophys. Sin. (Shanghai) 45, 2–10.

Srinivasan, S., 2015. Regulation of body fat in *Caenorhabditis elegans*. Annu. Rev. Physiol. 77, 161–178.

Taubert, S., Van Gilst, M.R., Hansen, M., Yamamoto, K.R., 2006. A Mediator subunit, MDT-15, integrates regulation of fatty acid metabolism by NHR-49-dependent and-independent pathways in *C. elegans*. Genes Dev. 20, 1137–1149.

Taylor, C.M., Wang, Q., Rosa, B.A., Huang, S.C.-C., Powell, K., Schedl, T., Pearce, E.J., Abubucker, S., Mitreva, M., 2013. Discovery of anthelmintic drug targets and drugs using chokepoints in nematode metabolic pathways. PLoS Pathog. 9, e1003505.

Urwin, P.E., Lilley, C.J., Atkinson, H.J., 2002. Ingestion of double-stranded RNA by preparasitic juvenile cyst nematodes leads to RNA interference. Mol. Plant Microbe Interact. 15, 747–752.

Van Gilst, M.R., Hadjivassiliou, H., Jolly, A., Yamamoto, K.R., 2005a. Nuclear hormone receptor NHR-49 controls fat consumption and fatty acid composition in *C. elegans*. PLoS Biol. 3, e53.

Van Gilst, M.R., Hadjivassiliou, H., Yamamoto, K.R., 2005b. A Caenorhabditis elegans nutrient response system partially dependent on nuclear receptor NHR-49. Proc. Natl. Acad. Sci. U.S.A. 102, 13496–13501.

Vanholme, B., De Meutter, J., Tytgat, T., Van Montagu, M., Coomans, A., Gheysen, G., 2004. Secretions of plant-parasitic nematodes: a molecular update. Gene 332, 13–27.

Walker, A.K., Yang, F., Jiang, K., Ji, J.-Y., Watts, J.L., Purushotham, A., Boss, O., Hirsch, M.L., Ribich, S., Smith, J.J., 2010. Conserved role of SIRT1 orthologs in fasting-dependent inhibition of the lipid/cholesterol regulator SREBP. Genes Dev. 24, 1403–1417.

Wallis, J.G., Watts, J.L., Browse, J., 2002. Polyunsaturated fatty acid synthesis: what will they think of next?. Trends Biochem. Sci. 27, 467–473.

Wanders, R., Ferdinandusse, S., Brites, P., Kemp, S., 2010. Peroxisomes, lipid metabolism and lipotoxicity. Biochim. Biophys. Acta, Mol. Cell. Biol. Lipids 1801, 272–280.

Watts, J.L., Browse, J., 2002. Genetic dissection of polyunsaturated fatty acid synthesis in *Caenorhabditis elegans*. Proc. Natl. Acad. Sci. U.S.A. 99, 5854.

Watts, J.L., Ristow, M., 2017. Lipid and Carbohydrate Metabolism in *Caenorhabditis elegans*. Genetics 207, 413–446.

Whitehead, A.G., Hemming, J.R., 1965. A comparison of some quantitative methods of extracting small vermiform nematodes from soil. Ann. Appl. Biol. 55, 25–38.

Yang, F., Vought, B.W., Satterlee, J.S., Walker, A.K., Jim Sun, Z.Y., Watts, J.L., DeBeaumont, R., Saito, R.M., Hyberts, S.G., Yang, S., Macol, C., Iyer, L., Tjian, R., van den Heuvel, S., Hart, A.C., Wagner, G., Naar, A.M., 2006. An ARC/Mediator subunit required for SREBP control of cholesterol and lipid homeostasis. Nature 442, 700–704.

You, Y.J., Kim, J., Raizen, D.M., Avery, L., 2008. Insulin, cGMP, and TGF-β signals regulate food intake and quiescence in C. elegans: a model for satiety. Cell Metabol. 7, 249–257.

Zambon, A.C., Gaj, S., Ho, I., Hanspers, K., Vranizan, K., Evelo, C.T., Conklin, B.R., Pico, A.R., Salomonis, N., 2012. GO-Elite: a flexible solution for pathway and ontology over-representation. Bioinformatics 28, 2209–2210.

Zhang, J., Bakheet, R., Parhar, R.S., Huang, C.-H., Hussain, M.M., Pan, X., Siddiqui, S.S., Hashmi, S., 2011. Regulation of fat storage and reproduction by Krüppel-like transcription factor KLF3 and fat-associated genes in *Caenorhabditis elegans*. J. Mol. Biol. 411, 537–553.

Zhang, Y., Zou, X., Ding, Y., Wang, H., Wu, X., Liang, B., 2013. Comparative genomics and functional study of lipid metabolic genes in *Caenorhabditis elegans*. BMC Genomics 14, 164.